ASSESSMENT OF LINEARIZED BUCKLING AND NONLINEAR BEHAVIOR OF COMPOSITE PANELS

Luciano Alves Martins, lalvmartins@gmail.com
Alfredo R. de Faria, arfaria@ita.br
Department of Mechanical Engineering, Instituto Tecnológico de Aeronáutica, CTA-ITA-IEM, São José dos Campos, SP 12228900

Abstract. *A conventional approach to the computation of critical loads of structures is to linearize the prebuckling state and to solve the resulting eigenproblem in order to obtain buckling loads as well as buckling modes. However, this approach is flawed, or extremely misleading, if in reality the prebuckling state is far from linear. Simple and useful structures, such as composite flat and cylindrical panels, have their buckling loads computed by traditional methods (linearized buckling). Nonlinear approaches are subsequently used to evaluate how realistic those linearized buckling loads are. Different stacking sequences are assessed in order to try to obtain information regarding the quality or realism of the linearized buckling loads. It is observed that for some laminates linearizing the prebuckling state leads to reasonable results. However, for other stacking sequences the results can be substantially inaccurate.*

Keywords*: Buckling, nonlinearity, composite materials*

1. INTRODUCTION

The assessment of buckling loads of panels is one of the most commonly used design criteria employed in the aerospace engineering practice. Usually the critical buckling loads are those obtained by techniques based on linearization of the prebuckling and, therefore, are applicable to situations where the loss of structural stability occurs through bifurcation, as in the case of flat panels free of initial imperfections. Nevertheless, most real aerospace structures have some degree of curvature or imperfection and, moreover, may buckle through limit point, what makes useless procedures based on linearization of the prebuckling state.

Real structures are not free of shape imperfections; a beam is slightly crooked, plates are not perfectly flat and shells exhibit similar deviations. In linear elastic analyses these imperfections (of small magnitude if compared to other dimensions of the structure) do not play a decisive role and can be neglected without detriment to the results. However, the shape imperfection effect is remarkable with respect to nonlinear stability theories.

After 1930 several researchers conducted experiments on axially compressed circular cylinders (Lundquist, 1933; Donnell, 1934). These experiments showed that the buckling loads were in severe disagreement with the theoretical predictions. The experimental results were as much as 70%-80% lower than the expected theoretical values. The reasons for this discrepancy were a controversial issue at the time. In 1945 Koiter (Koiter, 1970) demonstrated how initial imperfections can affect the equilibrium path of structures. His research remained relatively unknown until 1963 when his work was translated into English.

Even considering the simpler von Karman form of the nonlinear strains, the resulting equilibrium equations do not allow closed form solution. This is unfortunate since the nonlinear behavior of plates is fully described by these equations. Numerical methods have been used to solve the nonlinear equations for several load levels. Figure 1 shows the results for a plate subjected to edge load P. The amplitude of the lateral displacement w is the abscissa.

The bifurcation point is clearly seen where the primary and secondary paths meet. As the plate is loaded from $P = 0$, it remains on the primary path for reasonably small values of P. A secondary path originates when the critical load P_{cr} is reached. If P is further increased the plate turns to the secondary path which is stable (Roorda, 1986).

The path changes slightly in the presence of initial imperfections. The greater the magnitude of the imperfection, the farther the equilibrium path is from that of a perfect structure. Figure 1 shows that the plate is still capable of supporting loads after P_{cr} is reached.

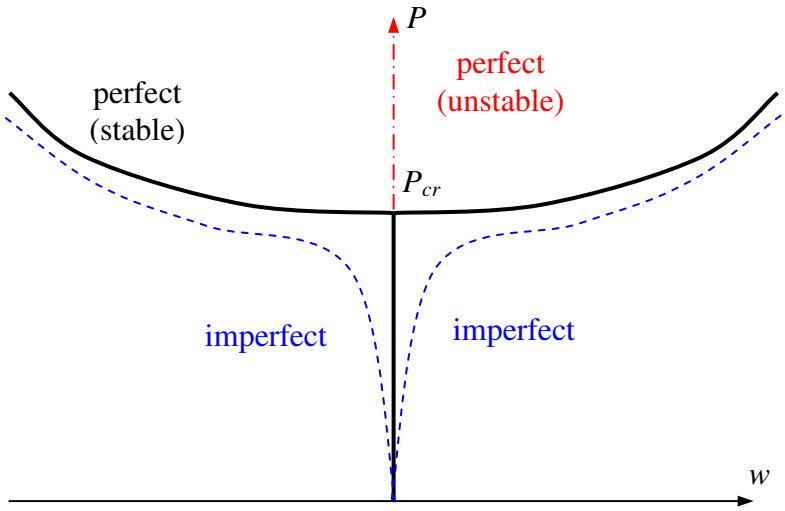

Figure 1. Nonlinear behavior of flat plates

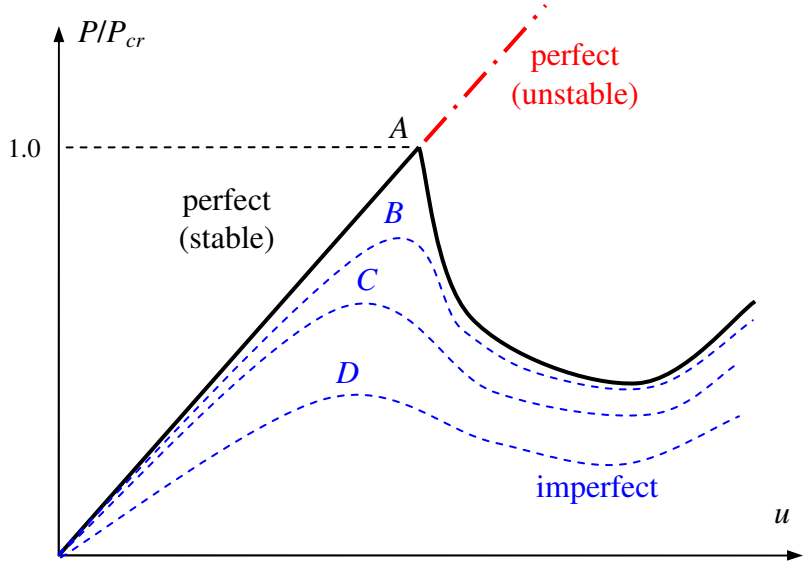

Figure 2. Nonlinear behavior of cylindrical panels

Comparing Fig. 1 with Fig. 2 (Brush and Almroth, 1975), where the nonlinear behavior of axially compressed cylindrical panels is shown, it is inferred that the initial imperfections produce a remarkable loss of strength in the postbuckling of cylindrical panels. The point where loss of stability occurs drops significantly when the imperfections increase (point $A \rightarrow$ point D). In general, whenever the slope of the secondary path at the bifurcation point is negative, the initial imperfections considerably reduce the structural resistance.

From the previous discussion on the effect of shape imperfections on the buckling of circular cylindrical panels it can be inferred that these structures possess a catastrophic postbuckling behaviour, i.e., its secondary path at the bifurcation point has negative slope. This means that cylinders, as opposed to flat plates, can no longer support load increments after the critical point is reached. Thus, every effort toward improvement of the critical load calculation is welcome and even more important than the flat plate case.

It is clear from Figs. 1 and 2 that the nonlinear response of initially imperfect structures can deviate significantly from the linearized response, what suggests that careless prebuckling linearization may lead to inaccurate results in some situations. It is noticeable that a bifurcation point, obtained from the linearized buckling eigenproblem, cannot be even identified when the nonlinearities involved in the structural response are severe. In this paper simple and useful structures, such as composite flat and cylindrical panels, have their buckling loads computed by traditional methods (linearized buckling) and nonlinear numerical methods are used to evaluate how realistic those loads are. Different stacking sequences are assessed in order to try to obtain some kind of preliminary information regarding the quality or realism of the linearized buckling loads.

2. A NUMERICAL METHOD FOR NONLINEAR PROBLEMS

The governing equations of equilibrium used to derive the principle of virtual work are inherently nonlinear. Even if the stress × strain relations are linear, the nonlinearity of the strain × displacement renders the equilibrium equations nonlinear. Therefore, an interactive and usually numerical procedure has to be used to find the equilibrium configuration.

It is possible to reformulate the principle of virtual work in terms of incremental displacements (Washizu, 1982). Suppose that the structure has reached an equilibrium configuration σ_{ij}, u_i, under the loads p_i, t_i., where σ_{ij} are components of the second Piola-Kirchhoff stress tensor, u_i are displacement components in a Cartesian reference system, p_i are components of the body force per unit volume and t_i are traction forces applied on the portion Γ_N of the boundary. Hence, the principle of virtual work reads

$$\int_{\Omega} \sigma_{ij}\delta\varepsilon_{ij}d\Omega - \int_{\Omega} p_i\delta u_i d\Omega - \int_{\Gamma_N} t_i\delta u_i d\Gamma = 0\,, \tag{1}$$

where Ω is the body domain, δ is the variational operator and

$$\varepsilon_{ij} = \frac{1}{2}(u_{i,j} + u_{j,i} + u_{k,i}u_{k,j}) \tag{2}$$

are the strain components.

The principle of virtual work can be reformulated in terms of incremental displacements (Washizu, 1982). Admit that the loads are perturbed by small quantities $\bar{p}_i$, $\bar{t}_i$ and, consequently, σ_{ij}, u_i are also perturbed by $\bar{\sigma}_{ij}$ and $\bar{u}_i$. The principle of virtual work now reads

$$\begin{aligned}&\frac{1}{2}\int_{\Omega}(\sigma_{ij}+\bar{\sigma}_{ij})[\delta u_{i,j}+\delta\bar{u}_{i,j}+\delta u_{j,i}+\delta\bar{u}_{j,i}+(\delta u_{k,i}+\delta\bar{u}_{k,i})(u_{k,j}+\bar{u}_{k,j})+\\&+(u_{k,i}+\bar{u}_{k,i})(\delta u_{k,j}+\delta\bar{u}_{k,j})]d\Omega-\int_{\Omega}(p_i+\bar{p}_i)(\delta u_i+\delta\bar{u}_i)d\Omega-\int_{\Gamma_N}(t_i+\bar{t}_i)(\delta u_i+\delta\bar{u}_i)d\Gamma=0\end{aligned}\,. \tag{3}$$

It is assumed that σ_{ij}, u_i is a known equilibrium configuration. Thus, $\delta\sigma_{ij}$, δu_i and their derivatives are zero yielding

$$\begin{aligned}&\frac{1}{2}\int_{\Omega}(\sigma_{ij}+\bar{\sigma}_{ij})[\delta\bar{u}_{i,j}+\delta\bar{u}_{j,i}+\delta\bar{u}_{k,i}(u_{k,j}+\bar{u}_{k,j})+(u_{k,i}+\bar{u}_{k,i})\delta\bar{u}_{k,j}]d\Omega-\\&\int_{\Omega}(p_i+\bar{p}_i)\delta\bar{u}_i d\Omega-\int_{\Gamma_N}(t_i+\bar{t}_i)\delta\bar{u}_i d\Gamma=0\end{aligned}\,. \tag{4}$$

Moreover, σ_{ij} and u_i is a state of equilibrium. Hence, Eq. (1) holds and since δu_i is arbitrary, they can be replaced by $\delta\bar{u}_i$ in Eq. (1) to give

$$\frac{1}{2}\int_{\Omega}\sigma_{ij}(\delta\bar{u}_{i,j}+\delta\bar{u}_{j,i}+\delta\bar{u}_{k,i}u_{k,j}+u_{k,i}\delta\bar{u}_{k,j})d\Omega-\int_{\Omega}p_i\delta\bar{u}_i d\Omega-\int_{\Gamma_N}t_i\delta\bar{u}_i d\Gamma=0\,, \tag{5}$$

Substituting Eq. (5) into Eq. (4),

$$\begin{aligned}&\frac{1}{2}\int_{\Omega}\sigma_{ij}(\delta\bar{u}_{k,i}\bar{u}_{k,j}+\bar{u}_{k,i}\delta\bar{u}_{k,j})d\Omega+\int_{\Omega}\bar{\sigma}_{ij}\delta\bar{\varepsilon}_{ij}d\Omega+\frac{1}{2}\int_{\Omega}\bar{\sigma}_{ij}(\delta\bar{u}_{k,i}\bar{u}_{k,j}+\bar{u}_{k,i}\delta\bar{u}_{k,j})d\Omega-\\&\int_{\Omega}\bar{p}_i\delta\bar{u}_i d\Omega-\int_{\Gamma_N}\bar{t}_i\delta\bar{u}_i d\Gamma=0\end{aligned}\,, \tag{6}$$

where

$$\bar{\varepsilon}_{ij} = \frac{1}{2}(\bar{u}_{i,j} + \bar{u}_{j,i} + \bar{u}_{k,i}u_{k,j} + u_{k,i}\bar{u}_{k,j}) . \tag{7}$$

Noticing that the third integral in Eq. (6) is one order above the others, it can be neglected. This third integral can be used to advantage as an error estimator in incremental procedures. Moreover, the second Piola-Kirchhoff stress tensor is symmetric ($\sigma_{ij} = \sigma_{ji}$) such that Eq. (6) becomes

$$\int_{\Omega} \sigma_{ij}\delta\bar{u}_{k,i}\bar{u}_{k,j}d\Omega + \int_{\Omega} \bar{\sigma}_{ij}\delta\bar{\varepsilon}_{ij}d\Omega - \int_{\Omega} \bar{p}_i\delta\bar{u}_i d\Omega - \int_{\Gamma_N} \bar{t}_i\delta\bar{u}_i d\Gamma = 0 . \tag{8}$$

Equation (8) can be understood as an incremental principle of virtual work. The first integral depends on σ_{ij} of the previous equilibrium state. The second integral depends on u_i because of Eq. (7). The term $\bar{\sigma}_{ij}$ can be linked to $\bar{\varepsilon}_{ij}$ considering the constitutive relation (Daniel and Ishai, 1990)

$$\sigma_{ij} = C_{ijkl}\varepsilon_{kl} . \tag{9}$$

Assuming that C_{ijkl} does not depend on the deformation state (purely geometrically nonlinear problem), the incremental constitutive relation, Eq. (9), becomes

$$\sigma_{ij} + \bar{\sigma}_{ij} = C_{ijkl}(\varepsilon_{kl} + \bar{\varepsilon}_{kl}) . \tag{10}$$

Combination of Eqs. (9) and (10) gives $\bar{\sigma}_{ij} = C_{ijkl}\bar{\varepsilon}_{kl}$, where the higher order term $\bar{u}_{k,i}\bar{u}_{k,j}$ has been neglected. Equations (8)–(10) consist of a linear system of equations in $\bar{u}_i$ that can be solved to obtain the incremental displacements. In the next iteration update the displacements to $u_i + \bar{u}_i$ and increase the loading to $p_i + \bar{p}_i$.

3. A PRELIMINARY EXAMPLE

Consider the shallow arc depicted in Fig. 3. Its ends are restricted in the *x* and *y* directions and a concentrated force *P* applied. The arc is made of an isotropic material whose mechanical properties are E = 200 GPa, ν = 0.3 and a thickness of 1.0 mm.

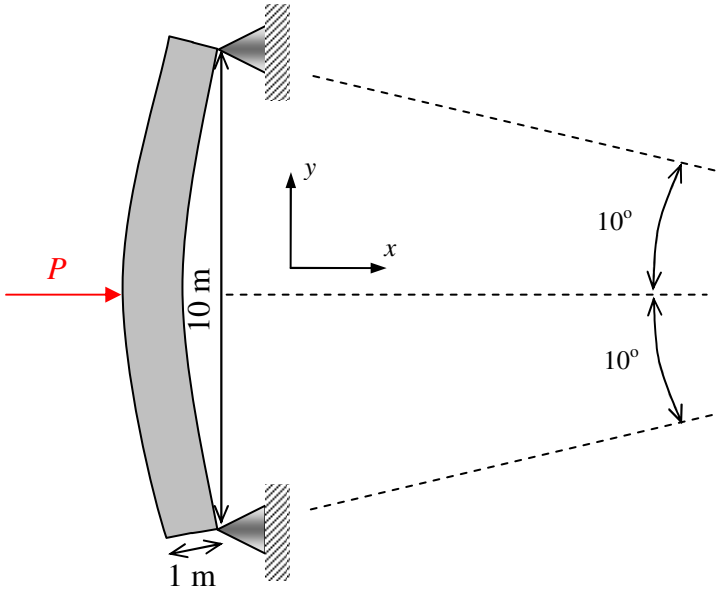

Figure 3. Shallow circular arc

The results of nonlinear simulations carried out according to the technique presented in the previous section and the commercial code MSC.Nastran are shown in Fig. 4, where the simulations have been stopped at $P_{cr} = 9.2\times10^5$ N. As expected (Brush and Almroth, 1975), a limit buckling point is observed. Loads above P_{cr} lead to instability and to a sudden jump to another stable equilibrium configuration. This jump cannot be computed using a force based numerical procedure. The alternative is to base the formulation on displacement what can be done by prescribing a displacement instead of a concentrated force. Another option is to use the arc length method that tries to avoid sudden jumps by restricting the length of the loading path that is covered from one load step to the next.

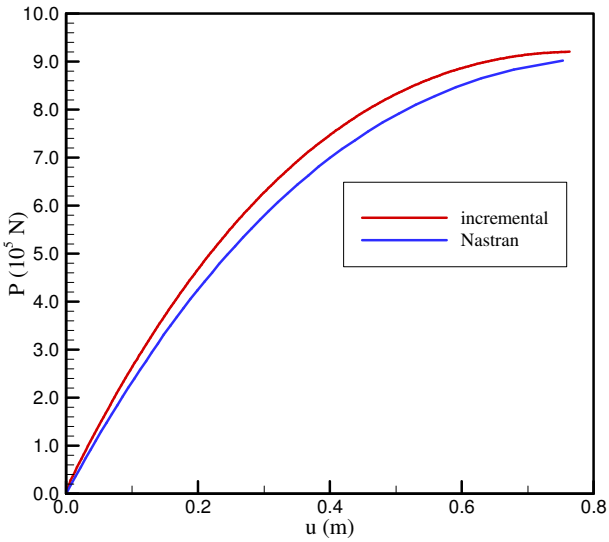

Figure 4. Shallow circular arc limit point

4. COMPOSITE PANEL RESULTS

The composite material adopted in the simulations has the following mechanical properties: $E_1 = 250$ GPa, $E_2 = 6.25$ GPa, $G_{12} = G_{13} = 6.125$ GPa, $G_{23} = 3.25$ GPa. Four symmetric laminates are considered: $[45/-45]_S$, $[0/90]_S$ and $[90/0]_S$. Each ply thickness is 1 mm.

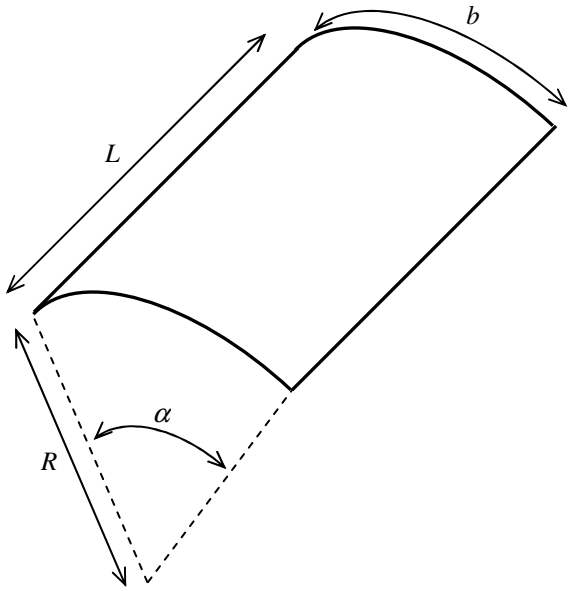

Figure 5. Cylindrical panel geometry

The panel geometry is depicted in Fig. 5, where R is the radius of the cylinder and α is the apperture angle. For the flat panel case $R = \infty$. In all simulations the panel length is assumed to be $L = 1$ m and the panel width is taken as $b = 1$ m. The boundary conditions consider that three edges (two straight edges and one circular) are pinned such that the three displacements are zero. The fourth edge (circular arc) is supported such that two displacements are zero and the

third is free to move in the direction along which the loading is applied (parallel to the straight edges). The load applied is uniformly distributed.

Initially linearized buckling analyses where conducted. The results are shown in Tab. 1 for different geometries and laminates. Finite element models of about 2,500 nodes were used in the simulations, what confers great accuracy to the numerical results obtained. The mesh density was defined by comparing the critical buckling load results for every mesh configuration, as the mesh density was increased. These analyses were performed on the flat panel and on the cylindrical panel with R = 0.5 m as shown in Fig. 6.

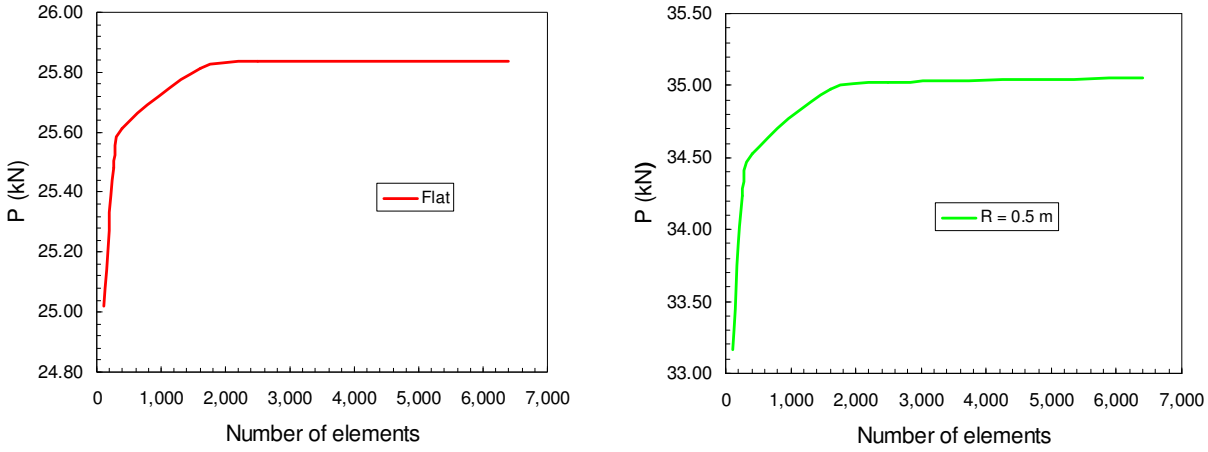

Figure 6. Mesh definition.

Table 1. Linearized buckling loads.

	$R = \infty$	R = 20 m	R = 10 m	R = 5 m	R = 0.5 m
$[45/-45]_S$	25.83 kN	25.84 kN	25.84 kN	25.87 kN	29.47 kN
$[0/90]_S$	12.80 kN	12.81 kN	12.80 kN	12.81 kN	14.35 kN
$[90/0]_S$	15.85 kN	15.87 kN	15.85 kN	15.85 kN	16.10 kN

It is interesting to notice that the classical buckling loads of the laminates considered are insensitive to variations in the panel curvature down to R = 5 m, which is a surprising conclusion. The linearized buckling loads increase substantially only when the curvature becomes pronounced (R = 0.5 m).

Nonlinear analyses for the flat panels are shown in Fig. 7. It can be noticed that the critical buckling loads computed in Tab. 1 are in good agreement with the behavior observed in Fig. 7, i.e., the highest buckling load is that for laminate $[45/-45]_S$. Two separate curves are shown in Fig. 7 because the scale in the x axis for the $[90/0]_S$ is incompatible with those for the $[45/-45]_S$ and the $[0/90]_S$ laminates.

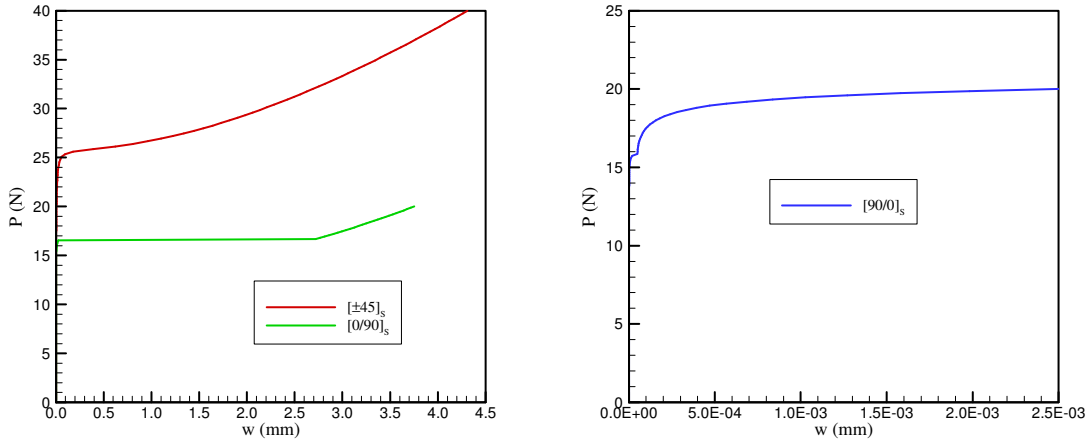

Figure 7. Nonlinear analyses: flat panel

Nonlinear analyses for the cylindrical panels with R = 20 m, R = 10 m, R = 5 m and R = 0.5 m are shown in Figs. 8, 9, 10 and 11 respectively. It can be noticed that the behavior is alike from those in Fig. 7. The general trend is the same

as in the flat panels case: the best nonlinear response is that for laminate $[45/-45]_S$. Observe, however, that the control displacement is now u rather than w.

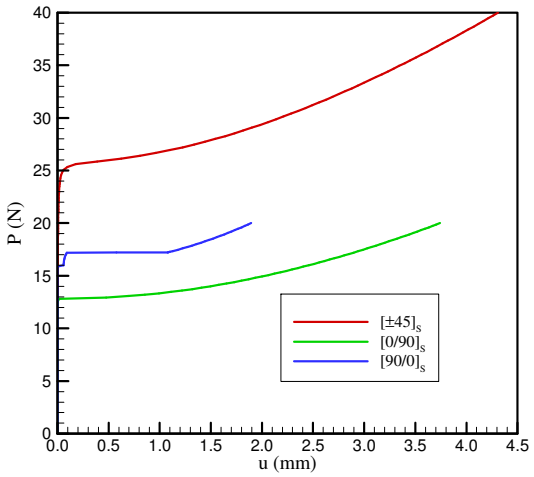

Figure 8. Nonlinear analyses: cylindrical panel (R = 20 m)

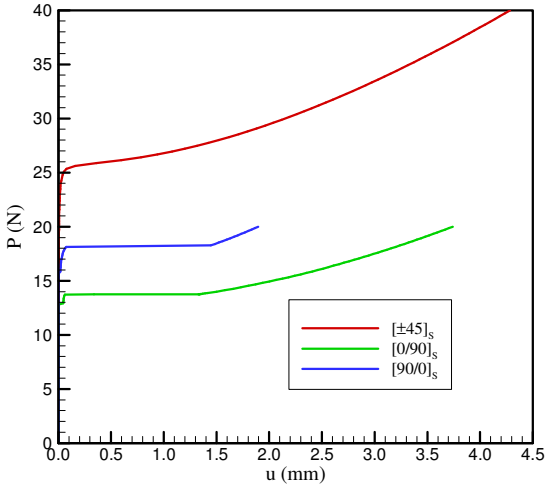

Figure 9. Nonlinear analyses: cylindrical panel (R = 10 m)

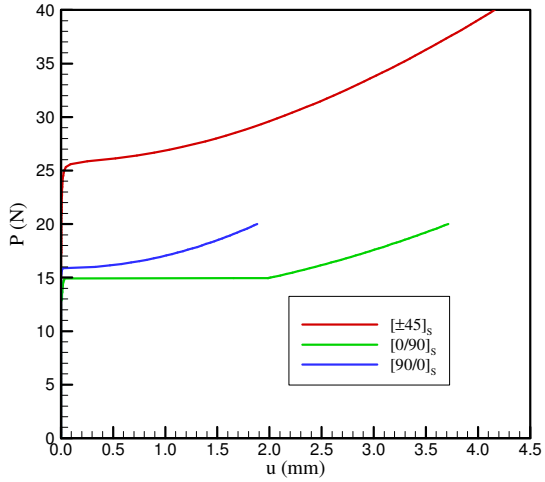

Figure 10. Nonlinear analyses: cylindrical panel (R = 5 m)

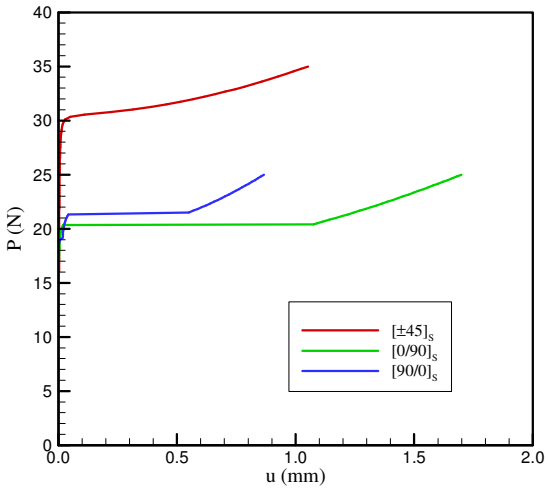

Figure 11. Nonlinear analyses: cylindrical panel (R = 0.5 m)

5. COMMENTS AND CONCLUSIONS

The nonlinear analyses conducted were extremely sensitive to the choice of numerical parameters. The steps of load applied were defined by increasing the increments until there was no more variation on the critical buckling load achieved.

The MSC.Nastran provides a default set of parameters to solve a non linear analysis, which includes a more suitable convergence method for the analyses chosen by the program and an update of the stiffness matrix every time the solution diverges or when it achieves its maximum iterations. This set of parameters led mostly to divergent solutions. Therefore, a full Newton-Raphson method was carried out, i.e. the stiffness matrix was updated at each step. This new set up generated much more accurate results, with no problems of convergence.

Although Figs. 7, 8, 9, 10 and 11 shows that the analyses continued after the determination of the critical buckling load, the results at post buckling cannot be considered as it is much more complex and requires some extra efforts and assumptions to be carried out.

This paper shows that for design purposes linearization of the buckling problem for flat and cylindrical panels lead to buckling loads is a good approximation of the real results.

It can be noticed that panels which present small variations of curvature can be approximated to a flat panel, as the results do not differ significantly. These analyses show that panel which present small curvature as a wing skin or horizontal stabilizer skin may be approximated to a flat panel. These small variations of curvatures could also represent small imperfections of panels, so it can be concluded that they do not influence much on the critical buckling load of the structure.

However fans of wind turbines for example, that present a significant curvature shall be analyzed as a cylindrical panel.

6. REFERENCES

Brush, D.O. and Almroth, B.O., 1975, “Buckling of Bars, Plates and Shells”, McGraw-Hill, New York.
Daniel, I.M. and Ishai, O., 1994, “Engineering Mechanics of Composite Materials”, Oxford University Press, NY.
Donell, L.H., 1934, “A New Theory for the Buckling of Thin Cylinders under Axial Compression and Bending”, ASME Transactions, vol. 56, pp. 795-806.
Koiter, W.T.,1970, “On theStability of Elastic Equilibrium”, Air Force Flight Dyn. Lab. Tech., report AFFDL-TR-70-25, Ferbuary.
Lundquist, E.E., 1933, “Strength Tests of Thin-walled Duraluminum Cylinders in Compression”, NACA report 473.
Roorda, J., 1986, “Buckling of Elastic Structures”, Solid Mechanics Division, University of Waterloo Press.
Washizu, K., 1982, “Variational Methods in Elasticity and Plasticity”, Pergamon Press, Oxford.

7. RESPONSIBILITY NOTICE

The authors are the only responsible for the material included in this paper.